Proc. Annual Meeting of the Austrian Society for Biomedical Engineering 2021
DOI: 10.3217/978-3-85125-826-4-19

PREDICTING EMG ENVELOPES OF GRASPING MOVEMENTS FROM EEG RECORDINGS USING UNSCENTED KALMAN FILTERING

A.I. Sburlea[1,*], N. Butturini[2,*], G.R. Müller-Putz[1]

[1]Instituteof Neural Engineering, Graz University of Technology, Austria
[2]University of Padova, Italy
[*]these authors contributed equally

gernot.mueller@tugraz.at

Abstract—*Electromyographic (EMG) control of prosthetics is well established both in research and clinical settings. However, it remains unclear how much of the EMG information can be predicted from the electroencephalographic (EEG) signals, and used instead, for control. In this study, we used a dataset that contains simultaneously acquired EEG and EMG signals of 31 subjects performing 33 grasping conditions, and applied unscented Kalman filtering (UKF) to continuously predict the EMG grasping envelopes from the low-frequency (0.1-2 Hz) EEG. We achieved higher prediction accuracy for intermediate grasps compared to power or precision grasps. Our findings indicate the feasibility of continuously predicting EMG envelopes of grasping movements from EEG signals.*

Keywords—*EEG, EMG, grasping, UKF*

Introduction

Electromyographic (EMG)-based control of prosthetic devices has shown to be reliable in the detection of the initiation of movement, as well as in identifying the desired grasping type [1, 2]. Currently, the prosthetic control achieved with EMG signals looks promising and it is in daily use for many amputees. However, this type of control faces some limitations when the number of functional muscles or neuromuscular content in the EMG signal are not sufficient (e.g., in the case of high amputation, such as shoulder exarticulation, or severe paralysis). One way of increasing performance is by leveraging the information related to the movement from the brain activity, in addition to the muscle information. Electroencephalographic (EEG) signals contain global motor-related information that can be accessed to predict, instead of merely responding to the user's intention. Recent EEG-based brain-computer interfacing (BCI) studies have shown the feasibility of discriminating between several types of movements [3-5]. Movement covariates, such as velocity of hand movement, have also been decoded from low-frequency EEG activity [6]. Furthermore, we have shown in a previous study that EEG and EMG activity share similarities during different stages of grasping [7]. Adaptive approaches for sensorimotor control have attracted a lot of attention over the last decades [8, 9]. Recent studies that use Kalman filtering approaches show promising results in terms of movement covariates' prediction from EEG activity [10, 11].

In this study, we investigated the feasibility of predicting the EMG envelopes of extrinsic hand muscles in a wide range of grasping movements from EEG signals. We conducted this study on a previously recorded dataset [7]. EEG and EMG activity were recorded simultaneously. We studied the amplitude patterns of the EEG signals in the delta frequency band (0.1-2 Hz) and used an unscented Kalman filter for the prediction. Our findings show the feasibility of this approach and could be informative for more intuitive and reliable upper-limb neuroprosthetic control.

Methods

A. Dataset description

A previously recorded dataset [7] has been used in this study. The dataset contains simultaneously acquired neural (EEG) and behavioral (muscle and kinematic) data of 31 participants, in a task that involves observation and execution of 33 different grasping movements. Figure 1A illustrates the structure of the experimental protocol.

During the fixation period, participants were instructed to focus their gaze on a cross located in the middle of the screen and avoid eye movements for three seconds. Next, during the observation phase which lasted four seconds, participants were presented with a static image showing a hand in a final grasping position together with the grasped object as shown in Figure 1B. During the execution phase which was also four seconds long, participants were instructed to focus their gaze on the "x" symbol located in the middle of the screen and perform the grasping movement that they had observed during the previous phase. Figure 1C shows the pictograms of the 33 grasping movements with their ordinal numbers. The order of the grasping conditions (blocks) was randomized among subjects.

EEG and electrooculographic (EOG) data was recorded using a 64-channel ActiCap System with two BrainAmp amplifiers (BrainProducts, Germany). The ground sensor was placed on AFz and the reference sensor on the right mastoid. Muscle activity was recorded with a Myo armband (Thalmic Labs Inc., Ontario, Canada). The armband was located on the right arm close to the elbow, above the extrinsic hand muscles.

Published by Verlag der TU Graz
Graz University of Technology

DOI: 10.3217/978-3-85125-826-4-19

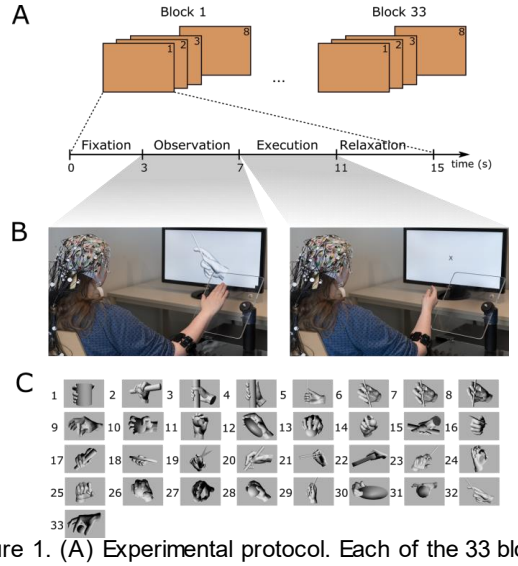

Figure 1. (A) Experimental protocol. Each of the 33 blocks contained eight consecutive repetitions (trials) of the same grasp. Each trial had four phases: fixation, observation, execution and relaxation. (B) Experimental setup. Photos of one participant during the observation and execution phases, and the materials used during recording. (C) Pictograms of the grasping conditions.

B. EEG and EMG data processing

For all data preprocessing and analyses, we used Matlab R2016b (Mathworks, Inc. USA). EEG data was first filtered using a Butterworth fourth-order, zero-phase, band-pass filter between 0.1–40 Hz and then downsampled to 100 Hz. We rejected the trials in which the task was incorrectly performed. From the EEG and EMG data we extracted 10-second long trials consisting of the last two seconds from the fixation period and the entire observation and execution periods. Next, we performed a similar cleaning processing pipeline as described in [7]. Then, we filtered the EEG data in the frequency range between 0.1–2 Hz using a zero-phase Butterworth band-pass filter of fourth-order. The eight EMG data channels were processed using Hilbert transform, standardized using z-score and, finally, the envelope of the data was computed. For both types of the data we reordered the groups of trials in a common order between subjects, as depicted in Figure 1C.

For each of the subjects we built an EEG-based measurement matrix by concatenating all the 10-second long trials, associated with different blocks of grasping conditions. In a similar way, the EMG data was concatenated across all trials to generate an EMG state vector (8 EMG channels by time samples for 264 trials, associated with 33 grasping conditions × 8 repetitions).

We used a hybrid approach similar to the one described in [12]. Like the standard Kalman filter, the n-th order unscented Kalman filter (UKF) [13] inferred the hidden state (the EMG envelope of the desired grasping) from the observations (low-frequency EEG amplitudes). The state transition model predicted the hidden state at the current time step given the state at the previous n time steps, where n is the order of the autoregressive model.

The standard Kalman filter is described by the following equations:

$$x_k = Fx_{k-1} + w_{k-1} \quad (1)$$

$$y_k = Hx_k + v_{k-1} \quad (2)$$

where the random variables w and v represent the process and measurement noise, respectively. They are assumed to be independent (of each other), white, and with normal probability distributions. The matrix F in (1) relates the state at the previous time step k-1 to the state at the current step k. The matrix H in (2) relates the state to the measurement. We choose a multivariate autoregression (MVAR) [14] to model the state transition equation because the trend of the EMG signal is assumed to be linear. The formula that describes the model is the following:

$$x_n = \sum_{i=1}^{m} x_{n-i} A_i(n) + e_n \quad (3)$$

where x_n is the nth sample of a d-dimensional time series, each $A_i(n)$ is a d-by-d matrix of coefficients (weights) and e_n is additive Gaussian noise. The neural tuning model relates the status of the system and the measures. To infer the relation between EEG and EMG signals we applied partial-least squares (PLS) as described in [15].

For each grasping condition, we performed an 8-fold cross validation (CV) among the EEG repetitions (7 trials for training and 1 trial for prediction). We used an n-th order UKF with a number of taps equal to the order of the fitted MVAR model (the model order was 3 or 4). For the PLS regression we have used the 10 previous lags of the EEG data to estimate the actual value of the EMG signal. Ten lags correspond to a time window equal to 0.4 s and we choose a fixed number of components (30), based on the level of explained variance (larger than 99%). Afterwards, we computed the mean over the different cross-validated predictions, for each trial and grasping condition.

C. Evaluation metrics

We define x_t as the measurement value and y_t as the prediction value at time t. We used Pearson correlation (r) and mean absolute error (MAE) to evaluate the quality of the EMG estimation with respect to the original EMG signal. Since MAE is a scale dependent metric, we expressed the prediction error in percentages and normalize it to the scale (the difference between maximum and minimum amplitudes) of the actual EMG envelope. We refer to the metric as normalized MAE (nMAE). The higher the r and the lower the nMAE values are, the better the prediction. Chance level values for our metrics were estimated by applying the 8-fold CV to shuffled data. We broke the association between x and y by randomly exchanging y across trials. The shuffling and 8-fold CV

Published by Verlag der TU Graz
Graz University of Technology

DOI: 10.3217/978-3-85125-826-4-19

procedure was repeated 100 times. Then, we then computed the α = 0.05 confidence interval for the r and nMAE distributions.
Next, we calculated the values of these two metrics for each EMG channel, grasp condition and subject. Finally, we present our prediction results for categories of grasps. Specifically, we group the 33 grasp conditions according to the more conventional grasping categorization into power, precision and intermediate grasp type, and according to the position of the thumb during grasping, adducted or abducted.

Results

A. Prediction accuracy of EMG envelopes

Figure 2 shows three cases of EMG envelope prediction. On the left plot we show an example of a good prediction (r = 0.65, nMAE = 20.4%), in which the overall shape of the predicted curve visually resembles the actual one. Similarly, the middle plot shows an average example of prediction (r = 0.41 and nMAE = 36.6%). In this case, the prediction is better during the grasping execution phase (from second 6 to 10) than in the other phases. Finally, the right plot shows an example of poor prediction (r = -0.13 and nMAE = 40%). In this example, the predicted signal captures the small EMG activation during the observation period, but fails to infer the muscle activation during the movement execution phase.

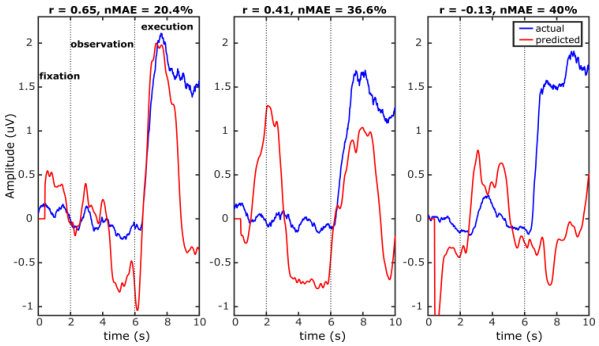

Figure 2. Examples of EMG single channel and single trial envelope estimation. Blue curves indicate actual EMG envelopes and red curves indicate predicted signals.

B. Correlation and normalized mean absolute error

Figure 3 shows median values of the two metrics for each grasping condition, across subjects. The highest r = 0.36 corresponds to grasp 11 (power sphere grasping), while the lowest nMAE value = 26% corresponds to grasp 16 (lateral grasping). We show the relation between all grasps relative to the two metrics of prediction. Dotted black lines indicate the overall median values for the two metrics. Dotted red lines show median chance level values across subjects and grasps. While it is informative to evaluate the prediction accuracy for each grasp, we believe that grouping the grasps into categories can be more interpretable and improve the general understanding of our findings. Hence, Figure 4 presents the results of the EMG envelope prediction for different categories of grasps. On the left side, the intermediate type of grasps has the lowest median nMAE = 27% compared to the power (nMAE = 28.7%) and precision (nMAE = 30.2%) types, and the highest correlation value r = 0.21, followed by r = 0.2 for power grasps and r = 0.18 for precision grasps. Regarding the categorization based on thumb's position, we found a better median prediction for the adducted grasps (r = 0.2, nMAE = 27.7%) than for the abducted grasps (r = 0.19, nMAE = 30%).

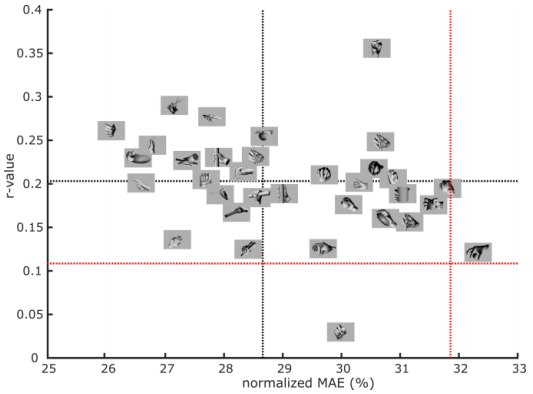

Figure 3. Scatter plot representation of all grasping conditions in terms of nMAE and r. The dotted black lines indicate the overall median values among grasping conditions for the two evaluation metrics: nMAE (vertical) and r (horizontal). The dotted red lines indicate the median chance level for the two metrics across subjects and grasps.

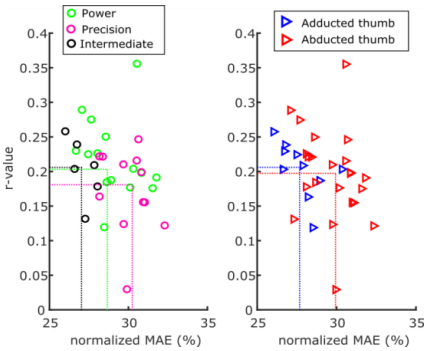

Figure 4. Prediction evaluation in terms of r and nMAE for two categorizations: Left. the type of grasp (power, precision and intermediate); Right. the position of the thumb (adducted and abducted). Dotted vertical and horizontal lines indicate median values for different groups of grasps.

Discussion

Our findings show the feasibility of predicting grasping EMG envelopes of extrinsic hand muscles from EEG signals using an UKF. In this study, we showed, for the first time, that EMG envelopes of a wide range of grasping conditions, involving periods of rest and movement, can be continuously predicted from low-frequency EEG amplitudes. Based on the presented categorizations of grasps we found a smaller predic-

Published by Verlag der TU Graz
Graz University of Technology

DOI: 10.3217/978-3-85125-826-4-19

tion error for the grasps in which the position of the thumb was adducted. Moreover, we observed that the EMG envelopes of intermediate grasps can be more successfully predicted from the brain activity, than power or precision grasps.

Previous studies have shown the ability of an UKF approach to infer EMG envelopes from low-frequency EEG amplitudes while performing a continuous ground walking task on different terrains [12, 16]. They obtained an overall r among subjects and muscles of 0.236, with an SNR of 0.8 dB. In the current study, we found a similar median r of 0.2 and an nMAE of 28.6%. However, a direct comparison between their findings and the ones of the current is not straightforward due to the differences in the performed task (other groups of muscles and different neural processes involved) and different number of movement repetitions.

Another study evaluated the prediction accuracy of grasping EMG envelopes of intrinsic hand muscles from firing rates in monkeys [17]. Their measurement consisted of more than 100 repetitions of each grasp leading to a better prediction and larger r than the ones reported in the current study. Nevertheless, comparison is again difficult due to further differences in signal acquisition modalities, measured hand muscles and signal processing.

Our findings show different levels of prediction accuracy among different grasps (Figure 3 and 4), as well as at single EMG channel level (Figure 2). We used median values to obtain robust global estimates in such cases of variability. Moreover, we employed r and nMAE as two complementary metrics for our prediction accuracy, evaluating both the phase and the amplitude similarity between the actual and the predicted values. Even though the number of grasps from each category is not the same, we observed that intermediate grasps have a lower median nMAE value than power or precision grasps. This observation could be due to the involvement of the wrist as an additional joint when performing intermediate grasp. Previous findings [3] have shown that EEG activity can be used to separate hand movements that involve different number of joints.

We have shown the feasibility of using UKF to predict grasping EMG envelopes from EEG activity; however, a better prediction could be achieved by increasing the number of movement repetitions for each grasp type, on which the model is trained. Moreover, the size of the prediction window plays also an important role, trading off precision to delay in the final prediction. In clinical setups, it is important to accommodate the delay between the EEG-based prediction and the actual triggering of the neuroprosthesis. Hence, different prediction windows could be evaluated in the future to enhance the control. These advances could lead to an intuitive and reliable interface that allows the user to reach autonomy in movement.

Acknowledgements

This research was supported by funding from the European Research Council (ERC-CoG 2015 681231 'Feel Your Reach').

References

[1] Ninu, A., *et al.* Closed-loop control of grasping with a myoelectric hand prosthesis: Which are the relevant feedback variables for force control?. *IEEE Transactions on Neural Systems and Rehabilitation Engineering, 22*(5), 1041-1052. (2014).

[2] Scheme, E. & Englehart, K. Electromyogram pattern recognition for control of powered upper-limb prostheses: state of the art and challenges for clinical use. *J. Rehabil. Res. Dev.* **48**, 643–659 (2011).

[3] Schwarz, A., *et al.* Decoding natural reach-and-grasp actions from human EEG. *J. Neural Eng.* **15**, 016005 (2018).

[4] Ofner, P., *et al.* Upper limb movements can be decoded from the time-domain of low-frequency EEG. *PLoS One* **12**, e0182578 (2017).

[5] Iturrate, I. *et al.* Human EEG reveals distinct neural correlates of power and precision grasping types. *Neuroimage* **181**, 635–644 (2018).

[6] Kobler, R. J., Sburlea, A. I. & Müller-Putz, G. R. Tuning characteristics of low-frequency EEG to positions and velocities in visuomotor and oculomotor tracking tasks. *Sci. Rep.* **8**, 17713 (2018).

[7] Sburlea, A. I. & Müller-Putz, G. R. Exploring representations of human grasping in neural, muscle and kinematic signals. *Sci. Rep.* **8**, 16669 (2018).

[8] Wolpert, D. M., Ghahramani, Z. & Jordan, M. I. An internal model for sensorimotor integration. *Science* **269**, 1880–1882 (1995).

[9] Antelis, J. M., *et al.* On the usage of linear regression models to reconstruct limb kinematics from low frequency EEG signals. *PLoS One* **8**, e61976 (2013).

[10] Schlögl, A., Vidaurre, C. & Müller, K.-R. Adaptive Methods in BCI Research - An Introductory Tutorial. *The Frontiers Collection* 331–355 (2009).

[11] Nakagome, S., *et al.* Prediction of EMG envelopes of multiple terrains over-ground walking from EEG signals using an unscented Kalman filter. in *2017 IEEE International Conference on Systems, Man, and Cybernetics (SMC)* (2017).

[12] Li, Z. *et al.* Unscented Kalman filter for brain-machine interfaces. *PLoS One* **4**, e6243 (2009).

[13] Wan, E. A. & Van Der Merwe, R. The unscented Kalman filter for nonlinear estimation. in *Proceedings of the IEEE 2000 Adaptive Systems for Signal Processing, Communications, and Control Symposium (Cat. No.00EX373)*

[14] Anderson, C. W., Stolz, E. A. & Shamsunder, S. Multivariate autoregressive models for classification of spontaneous electroencephalographic signals during mental tasks. *IEEE Transactions on Biomedical Engineering* **45**, 277–286 (1998).

[15] Ofner, P., & Müller-Putz, G.R. Using a noninvasive decoding method to classify rhythmic movement imaginations of the arm in two planes. *IEEE Transactions on Biomedical Engineering* 62.3 (2014): 972-981.

[16] He, Y. *et al.* An integrated neuro-robotic interface for stroke rehabilitation using the NASA X1 powered lower limb exoskeleton. *Conf. Proc. IEEE Eng. Med. Biol. Soc.* **2014**, 3985–3988 (2014).

[17] Ethier, C., *et al.* Restoration of grasp following paralysis through brain-controlled stimulation of muscles. *Nature* **485**, 368–371 (2012).

Published by Verlag der TU Graz
Graz University of Technology